NIH Public Access
Author Manuscript
Neuron. Author manuscript; available in PMC 2007 November 22.

Published in final edited form as:
Neuron. 2006 November 22; 52(4): 635–648.

Anomalous diffusion in Purkinje cell dendrites caused by spines

Fidel Santamaria[*], **Stefan Wils**[#], **Erik De Schutter**[#], and **George J. Augustine**[*]

***** *Department of Neurobiology, Duke University Medical Center, P.O. Box 3209, Durham, NC 27710 U.S.A.*

 # Laboratory of Theoretical Neurobiology, University of Antwerp, Belgium 2610

Abstract

We combined local photolysis of caged compounds with fluorescence imaging to visualize molecular diffusion within dendrites of cerebellar Purkinje cells. Diffusion of a volume marker, fluorescein dextran, within spiny dendrites was remarkably slow in comparison to its diffusion in smooth dendrites. Computer simulations indicate that this retardation is due to a transient trapping of molecules within dendritic spines, yielding anomalous diffusion. We considered the influence of spine trapping on the diffusion of calcium ions (Ca^{2+}) and inositol-1,4,5-triphospate (IP_3), two synaptic second messengers. Diffusion of IP_3 was strongly influenced by the presence of dendritic spines while Ca^{2+} was removed so rapidly that it could not diffuse far enough to be trapped. We conclude that an important function of dendritic spines may be to trap chemical signals and thereby create slowed anomalous diffusion within dendrites.

Keywords

chemical signaling; second messenger; Purkinje cell; chemical compartmentalization; calcium; IP_3

INTRODUCTION

Intracellular chemical signaling is critically important for regulating nearly all aspects of neuronal function, from transient changes in cell metabolism to long-lasting changes in synaptic transmission (Augustine et al., 2003;Wang and Storm, 2003;Bird et al., 2004). The degree of spatial and temporal localization of these chemical signals plays an important role in determining their ultimate course of action. This is particularly true for the case of neurons, whose complex structures can impart large influences on the generation and spread of chemical signals.

Here we consider this question by examining the influence of dendritic spines on diffusion. Spines are anatomical structures whose function has long been perplexing (Nimchinsky et al., 2002). It is widely thought that spines serve to compartmentalize chemical signals generated by synaptic activity, thereby impeding diffusion of these signals into dendrites (Sabatini et al., 2001). A substantial amount of experimental data supports this hypothesis (Yuste et al., 1999;Ngo-Anh et al., 2005;Sobczyk et al., 2005), particularly for short-lived signals such as

Please address correspondence to G. Augustine: georgea@neuro.duke.edu

Diffusion of chemical signals is an essential component of neuronal signal transduction. Combining computer simulations and imaging techniques reveals that molecules in Purkinje cell dendrites undergo a slowed form of diffusion, called anomalous diffusion, due to transient trapping of molecules in spines. Anomalous diffusion results from an increase in the spatial and temporal correlation of trapped molecules inside spines, which could exert an important influence on signal transduction in dendrites and their spines.

Publisher's Disclaimer: This is a PDF file of an unedited manuscript that has been accepted for publication. As a service to our customers we are providing this early version of the manuscript. The manuscript will undergo copyediting, typesetting, and review of the resulting proof before it is published in its final citable form. Please note that during the production process errors may be discovered which could affect the content, and all legal disclaimers that apply to the journal pertain.

NIH-PA Author Manuscript
NIH-PA Author Manuscript
NIH-PA Author Manuscript

NIH-PA Author Manuscript

NIH-PA Author Manuscript

NIH-PA Author Manuscript

calcium ions (Ca^{2+}), though there are also indications that this may not always be the case (Miyata et al., 2000;Holthoff et al., 2002;Noguchi et al., 2005).

We have addressed this problem from a different perspective, asking whether spines influence the diffusion of chemical signals along dendrites. Purkinje cells (PCs) are a good system in which to study this question because their dendrites contain both sections without spines, as well as branches with high densities of spines (Palay and Chan-Palay, 1974;Harris and Stevens, 1988). We found that a biologically inert compound, fluorescein dextran (FD), exhibits different diffusion properties in these two types of dendrites, with diffusion being slower and non-linear within spiny dendrites. Computational modeling indicates that this difference arises because spines act as temporary traps for molecules as they move along spiny dendrites, yielding a process known as “anomalous” diffusion that is physically distinct from conventional diffusion (Klafter and Sokolov, 2005). Other experiments demonstrate that Ca^{2+} ions are strongly buffered, so they are removed before being trapped by spines, while inositol-1,4,5-trisphosphate (IP_3) is trapped much more as it diffuses through dendrites. Because anomalous diffusion also causes molecules to be correlated in space and in time, trapping may influence signal transduction within spines.

RESULTS

The goal of this study was to determine the influence of dendritic spines on diffusion of molecules within PC dendrites. We began by uncaging FD, an inert tracer whose diffusion should be limited only by cellular geometry. A brief flash of UV light (5 ms in duration, 3–8 μJ energy) was used to uncage FD within a small spot (7 μm half-width) within PC dendrites (Wang and Augustine, 1995). The resulting change in FD fluorescence ($\Delta F/F_o$) was tracked at high speed (120 images per second) to examine the diffusional redistribution of FD over time. Representative images from such an experiment are shown in Fig. 1A. The top image shows the fluorescence of Texas Red, a non-caged dye that was introduced into the PC to visualize dendritic structure. The three lower images show superimposed pseudocolor overlays of $\Delta F/F_o$ at three different times. Changes in FD fluorescence reached a maximum within 50 ms of the light flash (arrowhead, Fig. 1B). To avoid possible complications due to the finite time required for caged FD to be uncaged, we began our analysis at the time when FD fluorescence was maximal (t = 0). Bleaching reduced FD fluorescence by less than 30% over 1 s (Fig. 1B).

As is evident in the images of Fig. 1A, diffusion of FD was remarkably slow in spiny dendrites. Such behavior is analyzed in Fig. 1C, which shows the corresponding spatial profiles of FD along the dendritic path indicated by the blue line in Fig. 1A. At t = 0, FD fluorescence was distributed in a Gaussian profile and the width of this profile changed relatively little over the next second. To examine the time course of diffusional redistribution of FD, the spatial variance of FD fluorescence at each time point was calculated from plots such as those in Fig. 1C using eq. 13 (see Methods). This variance did not increase linearly over time, as expected for normal diffusion (eq. 12), but instead showed strong non-linear properties (Fig. 1D). These measurements of spatial variance allowed us to use eq. 14 to determine the instantaneous apparent diffusion coefficient (D_{app}) of FD at each time point. These values were normalized by the diffusion coefficient of FD measured in intracellular solution (D_{free} = 0.08 $\mu m^2/ms$), yielding a parameter that illustrates the time-dependent retardation of FD diffusion within the PC (Fig. 1E). The initial value of the D_{app} was close to 40% of that of D_{free} and D_{app} decayed further throughout the duration of the measurements. Note that this decay was not due to bleaching of FD, because it was not correlated with the time course of bleaching (Fig. 1B); in any case, bleaching affects fluorescence uniformly along the dendrite and should not change the spatial distribution of FD fluorescence. Instead, this time-dependent decay in the D_{app} indicates the presence of a process that progressively slows diffusion of FD.

NIH-PA Author Manuscript

NIH-PA Author Manuscript

NIH-PA Author Manuscript

Modeling diffusion in dendrites

We next used computational models of intracellular diffusion to understand how the structure of PCs might slow the diffusion of an inert molecule such as FD. Our simulations were based on the conditions of experiments, such as the one in Fig. 1, where molecules with D_{free} equal to that of FD were introduced within a volume that initially occupied a 1–3 μm long segment of a cylindrical dendrite. The dendrite had a total length of 120 μm and a radius of 0.2–8 μm.

Our simulations first considered a smooth dendrite without spines. As expected, the variance of the spatial distribution was linearly dependent on time and D_{app} was constant over time (Supplementary Material Fig. S1). This is consistent with simple diffusion but differs from the behavior observed in PC dendrites (Fig. 1E). Diffusion in this simple structure has an analytical solution (Crank, 1975), allowing us to validate the results from our numerical simulation. The model closely matched the analytical solution, with differences between the calculated and predicted D_{app} being less than 1%. The consistency between the predictions of our model and the analytical solutions indicates that boundary effects due to the finite length of the cylinder and reflective walls have no significant influence on our results, at least for times up to 1 s.

We next considered what causes diffusion of FD in PC dendrites to be so different from that expected in a simple, cylindrical dendrite. Because FD is not bound within PC cytoplasm or transported out of the PC, the complex structure of the PC dendrite is a likely source of this difference. Simulations indicate that many aspects of this structure, such as the presence of many branches and changes in taper, have relatively small influences on D_{app} (Figs. S2 and S3). However, dendritic spines are present at a very high density on PCs (Harvey and Napper, 1991) and these were predicted to have very significant effects. We considered the effect of dendritic spines by randomly inserting spines along an unbranched dendrite. Each spine consisted of two concentric cylinders representing neck and head compartments (Fig. 2A). The sizes of these compartments were randomly varied within the range of published values (Harris and Stevens, 1988; see Methods), so that neck diameters varied from 0.1–0.3 μm, while neck lengths ranged from 0.4–2.1 μm and head lengths were between 0.4–0.7 μm. Spine head diameter depended upon the values of head length and volume and ranged from 0.5–0.7 μm, with a minimum ratio of head-to-neck diameter of 1.5. In all cases the total volume of the neck and head were within the range of values reported by Harris and Stevens (1988). D_{app} was then determined for molecules diffusing along the main dendrite, to simulate experimental measurements such as those in Fig. 1.

This model predicted that spines dramatically slow diffusion within dendrites. By varying the density of spines, we found that increasing spine density had progressively greater effects on spread along the dendrite (Fig. 2B). Higher spine density was also predicted to decrease spatial variance non-linearly over time (Fig. 2C), with the non-linear time dependence clearest at earlier times (Fig. 2D). This behavior reflects what was observed in the measurements of FD spread in PCs (Fig. 1D). The non-linear behavior of spatial variance over time was also reflected in a time-dependent reduction in D_{app}, which continuously decreased over time and did not reach a stable value within 1 sec (Fig. 2E). The fraction of volume occupied by the spines increased with higher spine density, resulting in a lower fraction of molecules moving along the dendrite. However, this was not the sole cause of the time-dependent reduction in D_{app} because the fraction of molecules remaining in the dendrite reached a constant value in less than 100 ms (Fig. S4) while D_{app} continued to decline for at least 1 sec. At a density of 10–13 spines/μm, which is typical for 1 μm diameter dendrites in PCs (Harvey and Napper, 1991), D_{app} was predicted to decay by 50% within 200 ms (Fig. 2E), which is very similar to what was observed in living PCs (Fig. 1E).

The sub-linear changes in spatial variance over time that are illustrated in Figs. 2C and D can be characterized by a power law of the form:

NIH-PA Author Manuscript

NIH-PA Author Manuscript

NIH-PA Author Manuscript

$$< x^2 > \alpha D_o * t^{2/d_w} \quad (1)$$

where $<x^2>$ is the spatial variance, t is the time and D_o is the diffusion coefficient. If the exponent, d_w, of this function is 2, then the process is considered to be normal diffusion (eq. 12). However, if $d_w>2$, then the process is called *anomalous diffusion* (ben-Avraham and Havlin, 2000). For this reason, we will refer to d_w as the anomalous exponent. Anomalous diffusion arises when the random walk performed by molecules is influenced by their previous positions in space (Klafter and Sokolov, 2005). This makes the process of anomalous diffusion mechanistically quite different from that of normal diffusion, where the movement of a particle is independent of its previous position. Given the relationship between $<x^2>$ and D_o, eq. 1 indicates that the diffusion coefficient depends on time and can be rearranged to yield:

$$< x^2 > \alpha D(t) * t \quad (2)$$

where D(t), the time-dependent diffusion coefficient, is

$$D(t) = D_o * t^{2/d_w - 1} \quad (3)$$

From eq. 3, d_w can be obtained graphically from the inverse of the slope (m) of logarithmic plots of $(<x^2>/t)$ over time:

$$d_w = 2 / (m + 1) \quad (4)$$

Fig. 3A shows such a logarithmic transform of the simulation results shown in Fig. 2C, sampled and averaged as in the experiments (see Fig. 4). To compare the anomalous portion of this and subsequent plots, we referenced them to a value of 0 at early times. The horizontal line, with a slope of 0, corresponds to normal diffusion ($d_w = 2$). This line also represents the simulation results for the case of a dendrite without spines, which exhibited normal diffusion. In cases where dendritic spines were added, the function decayed slowly over the first several ms, during which diffusion was almost normal. After this initial delay, the function decreased steeply beginning at 20 ms and continued to decline for as long as 500 ms, with the steepness of this decline proportional to the density of spines. Linear fits to points within this section of the curves (thick lines) were used to calculate the anomalous exponent and indicate that d_w increased linearly with spine density (Fig. 3B). The values of d_w were calculated for two different values of D_{free} (0.08 μm^2/ms, filled symbols; 0.2 μm^2/ms, open symbols) and d_w was found to be independent of D_{free}. This indicates that anomalous diffusion is due to the structure of the dendrite, rather than the nature of the diffusing particles, which is a characteristic property of anomalous diffusion (Saxton and Jacobson, 1997).

At later times, the slope of the functions declined as diffusion returned to a normal process, albeit with a reduced rate. Such a transition from anomalous diffusion to reduced normal diffusion is commonly observed when particles move through randomly scattered obstacles (Saxton, 1994) or are trapped in a time-dependent fashion (Ritchie et al., 2003; ben-Avraham and Havlin, 2000). Depending on the density and depth of these traps (in our case the shape and size of the spine; see below), molecules can undergo both types of diffusion, with anomalous diffusion usually having a stronger influence at shorter times. Over a wide range of physiologically relevant values of D_{free} and spine densities, it was rare for diffusion to return to a flat slope, indicating reduced normal diffusion, before 1 s. In fact, extending to 1 s the linear fits for the curves generated with 5–15 spines/μm changed the value of d_w by less than 7%. Therefore, our simulations suggest that, within the time window of our experiments,

NIH-PA Author Manuscript

NIH-PA Author Manuscript

NIH-PA Author Manuscript

molecular movement within dendrites is dominated by anomalous diffusion and that this anomalous diffusion is caused by the presence of dendritic spines.

These simulations indicate that dendritic spines can act as traps for molecules diffusing along a dendrite. The brief delay apparent in the plots of Fig. 3A would then reflect the time required for these molecules to reach (and be trapped) by spines. When there are no spines (Fig. 3C, top), molecules will diffuse freely, except for reflecting off the plasma membrane, yielding a normal diffusion process. When spines are present (Fig. 3C, middle), molecules have some probability of entering the spines and remaining trapped for a while before returning to the dendrite to diffuse freely. Anomalous diffusion in dendrites is therefore a dynamic process, originating from the fact that molecules can both enter and leave spines. It is very different from the 'capacitative' effect that would occur if trapped molecules could not leave the spine (Zador and Koch, 1994); such an effect would have resulted in normal diffusion, with a reduced D_{app} that was constant over time. In the extreme case of very high spine density, molecules that leave a spine will have a high probability of entering another spine. This will dramatically limit axial displacement of molecules along the dendrite, so that they effectively will be unable to move away from their sites of generation (Fig. 3C, bottom). This condition is referred to as the percolation limit (Saxton and Jacobson, 1997) and is evident in logarithmic plots as a line with a slope that approaches -1 as d_w approaches infinity (Fig. 3A, dashed line).

Spine-induced anomalous diffusion was predicted to depend upon the geometry of the spines. This was evaluated systematically, at a fixed spine density (15 spines/μm), using the average values for spine parameters (0.2 μm neck diameter, 0.6 μm neck length, and 0.6 μm head diameter and length). We varied the length and diameter of the spine head and neck within the ranges reported for PCs (Harris and Stevens, 1988), while keeping the remaining parameters constant. The structural parameter that had the largest influence on d_w was the diameter of the spine head (Fig. 4A), while variations in the length of the spine head or neck had little influence (data not shown). Because the volume of the spine increased when the diameter of the spine head was varied, it is possible that d_w increased because of spine volume changes. However, this was not the case because increasing the volume of a spine alone had minimal effects on d_w (Fig. 4B). Further, the effects of increasing the fractional volume occupied by spines should reach equilibrium in less than 100 ms (Fig. S4), while anomalous diffusion lasted much longer (Figs. 2E and 3A). A similar outcome was obtained when the spine volume was kept fixed as spine diameter and length were varied (Fig. 4C). However, when the spine neck parameters were fixed and the volume of the head was constant, d_w still increased as the head diameter increased (Fig. 4D). Therefore, the parameter that regulates d_w is the size of the head with respect to the neck. Our interpretation is that spine trapping relies on the properties of the "bottleneck" between the head and shaft of the spine. The flattening of the curve in Fig. 4D at large values of head diameter presumably results from the spine head becoming very short, increasing the probability that molecules reflect off the top of the spine head and return to the spine neck.

Anomalous diffusion in Purkinje cell spiny dendrites

Our modeling results indicate that the presence of dendritic spines should generate anomalous diffusion in dendrites. We tested this possibility experimentally by comparing the spread of FD fluorescence signals in spiny and smooth dendrites of living PCs. Fig. 5A shows a composite image of two uncaging episodes performed in the same PC, one at a smooth dendrite and the other at a spiny dendrite. We analyzed the fluorescence profiles and their spatial spread along the indicated paths, as in Figs. 1C and D, and found considerable differences between diffusion in the two regions of the dendrite (Figs. 5B–D). The logarithmic transformation illustrated in Fig. 3A was used to plot the time-dependent decline in FD fluorescence in the two dendrites. This transformation revealed that the spread of FD could be described as an

NIH-PA Author Manuscript

NIH-PA Author Manuscript

NIH-PA Author Manuscript

anomalous diffusion process for times as long as 1 s for the spiny dendrite, while diffusion in the smooth dendrite was less anomalous. Fits to the linear portion of these functions (Fig. 5E) were used to determine d_w, which in this case was 2.6±0.1 (95% confidence intervals of linear fit) for the smooth dendrite and 4.6±0.6 for the spiny dendrite. Thus, as predicted by our simulations, spread of FD in spiny PC dendrites behaves like an anomalous diffusion process, while diffusion in smooth dendrites is nearly normal.

We calculated d_w for smooth and spiny dendrites in a total of 21 measurements taken from 6 different cells. The top panel in Fig. 6A shows logarithmic plots for all the data, separated into spiny (red) and smooth (black) dendrites, and the bottom panel shows their averages. The results of individual experiments indicated that in every case where FD was uncaged in spiny dendrites, anomalous diffusion was present throughout the entire duration of the measurement. In smooth dendrites, only normal diffusion was observed in 3 experiments (upper 3 black curves in Fig. 6A, top), while in the remaining 5 experiments a small amount of anomalous diffusion was evident. On average, while spiny dendrites had a d_w of 8.0±1.4 (S.E.M.), smooth dendrites had a d_w of 3.0±0.2, which is close to the value of 2 associated with simple diffusion (Fig. 6B). Because the average diameter of smooth dendrites is larger than that of spiny dendrites in PCs (Gundappa-Sulur et al., 1999), we also calculated d_w for cases where these two types of dendrites had comparable diameters (1.5 to 3.5 μm). For this subset of smooth dendrites the mean d_w (3.1±0.2 S.E.M.) again was significantly smaller ($p<0.05$, t-test) than that of spiny dendrites (6.9±1.0). Although the average dendritic length of spiny (18.0±1.6 μm S.E.M) and smooth (31.1±2.0 μm) dendrites was different, the correlation between d_w and the length of spiny dendrites was small ($r = 0.33$) and insignificant ($p = 0.32$). Thus, differences between diffusion in the two types of dendrites were not due to differences in diameter or length. Instead, anomalous diffusion was associated with the presence of dendritic spines, as predicted by our simulations.

We considered alternative explanations for the occurrence of anomalous diffusion of FD in spiny dendrites. One possibility is that bleaching of FD could produce a time-dependent loss of fluorescence that would resemble anomalous diffusion. However, anomalous diffusion was observed at times when FD bleaching was minimal (Figs. 1B and S5) and calculations indicated that the small amount of FD bleaching that was present could not produce anomalous diffusion behavior (Fig. S6D). These considerations dismiss bleaching as a cause of the anomalous diffusion of FD. We also asked whether the finite length of the dendrite segments analyzed would cause a time-dependent loss of dye from the end of the dendrite that resembled anomalous diffusion. Three arguments indicate that this is not the case: (1) Our measurements did not show any decay in fluorescence that could account for the observed reductions in apparent diffusion (see Figs. S5 and S6). (2) Calculation of the spread of a concentration profile is independent of its amplitude, so that a homogeneous disappearance of molecules along dendrites would only scale the amplitude of the fluorescent profiles without changing their apparent spread. (3) Calculations indicate that such effects would not yield the behavior measured experimentally (Fig. S6C). These arguments also dismiss the possibility that the anomalous diffusion behavior arises from movement of dye to dendritic branches other than the ones analyzed. Thus, we conclude that FD exhibits anomalous diffusion in spiny dendrites of PCs.

Although the simulations we implemented are simplified cases, the values of d_w measured in living PCs usually were within the range obtained in the simulations. While our simulations predicted values of d_w between 2–6 in spiny dendrites, values of d_w were between 3.2–7.0 in 7 out of 11 experimental measurements in PCs. Remaining differences between the simulations and experimental measurements could result from several factors, such as higher spine densities and/or larger spine volumes (Harris and Stevens, 1988) or from contributions from intracellular organelles, such as endoplasmic reticulum (Martone et al., 1993;Weiss et al.,

NIH-PA Author Manuscript

NIH-PA Author Manuscript

NIH-PA Author Manuscript

2004). In particular, the presence of intracellular organelles could explain why the values of d_w in smooth dendrites were somewhat above the value of 2 expected for free diffusion.

The striking difference in the reduction of the spatial spread between the spiny and smooth dendrites could not be accounted for by other structural differences, such as the dimensions or branching patterns of the dendrite, because the model predicts that these parameters will have relatively small effects on diffusion (Fig. S2 and S3). The predictions of these simplified models were confirmed and extended by first reconstructing the dendrites of the PC shown in Fig. 5 and then simulating diffusion within this complex structure under various conditions. The effects of dendrite branching were considered by simulating diffusion in the main smooth dendrite and comparing diffusion in the presence and absence of side branches (Fig. 7A). These simulations indicated that branching had little effect, evident as minimal effects on both the time course of the spatial variance (Fig. 7B left) and on the logarithmic transform of the variance (Fig. 7B right). The influence of spines was considered by simulating diffusion in the spiny dendrite in the absence or presence of spines (Fig. 7C).

The presence of spines caused a time-dependent reduction in spatial variance (Fig. 7D left) and increased d_w from a value of 2.3, indicating near-normal diffusion, to 3.8, indicating anomalous diffusion (Fig. 7D right). The small non-linear time-dependence of variance apparent in the smooth dendrite could be distinguished from anomalous diffusion because it did not show a power law relationship, i.e., a straight oblique line on the logarithmic plot (Fig. 7D right). This behavior presumably arose from the time-dependent loss of molecules into other dendrites, as illustrated in Fig. S6C. These anatomically realistic simulations indicate that it is the presence of spines - rather than the finite length or branching pattern of the dendrite - that generates anomalous diffusion in spiny dendrites of PCs.

Anomalous diffusion limits spread of second messengers

The above results indicate that dendritic spines slow diffusion of FD in dendrites. We next sought to determine whether similar anomalous diffusion processes could limit the intracellular spread of physiological signals, such as second messengers. We first considered Ca^{2+}, a second messenger important for the control of ion channels (Edgerton and Reinhart, 2003;Womack et al., 2004) and synaptic efficacy (Hartmann and Konnerth, 2005) in PC dendrites. Calcium is tightly controlled within PCs (Fierro and Llano, 1996;Maeda et al., 1999) due to the presence of numerous calcium-binding proteins (Maeda et al., 1999;Schmidt et al., 2003) and Ca^{2+} pumps (Sepulveda et al., 2004;Hartmann and Konnerth, 2005), allowing us to consider an extreme case where spread is limited by cellular regulatory mechanisms.

Local rises in intracellular Ca^{2+} concentration ($[Ca^{2+}]_i$) were produced by focal photolysis of DMNPE-4, a caged Ca^{2+} compound (Ellis-Davies, 1998). The resulting changes in $[Ca^{2+}]_i$ were monitored with a fluorescent indicator dye, Oregon Green BAPTA-1 (Finch and Augustine, 1998), as shown in Fig. 8A. In contrast to the fluorescence signals associated with uncaging of FD (Fig. 1B), fluorescence signals associated with local $[Ca^{2+}]_i$ changes were short-lived and returned to basal levels in less than 500 ms (Fig. 8B). This rapid decay is presumably due to efficient removal of Ca^{2+} by buffers and pumps. The spatial profile of fluorescence changes within the dendrite, along the path indicated by the blue line in Fig. 8A, is shown in Fig. 8C. In 9 experiments from 8 cells, spatial variance increased only a small amount over time (Fig. 8D). For both spiny and smooth dendrites, this time-dependent increase in variance was linear, with a slight trend toward slower increases in spiny dendrites than in smooth dendrites. The slope of the plots in Fig. 8D correspond to a D_o of 0.32±0.11 μm^2/ms (95% confidence interval of the fit) for smooth dendrites and 0.21±0.04 μm^2/ms for spiny dendrites. Because these diffusion coefficients are too fast for buffered Ca^{2+} diffusion (0.065 μm^2/ms, Allbritton et al., 1992), they are likely to reflect movement of the indicator dye (Neher and Augustine, 1992) and are in good agreement with the diffusion coefficient of 0.2 μm^2/ms

NIH-PA Author Manuscript

NIH-PA Author Manuscript

NIH-PA Author Manuscript

for calcium dyes (Michailova et al., 2002). Logarithmic plots of variance/t over time indicate a lack of anomalous diffusion, with d_w approaching 2 (Fig. 8E). These results indicate that diffusion of Ca^{2+} is very limited – presumably due to the robust Ca^{2+} removal mechanisms of PCs (Fierro et al. 1998;Maeda et al., 1999;Schmidt et al., 2003;Sepulveda et al., 2004) - but appears to be almost linear for the brief time that the signal lasts. Assuming a diffusion coefficient for Ca^{2+} of 0.065 μm^2/ms (Allbritton et al., 1992), a decay time constant of 120 ms would prevent Ca^{2+} from spreading more than 5 μm from the site of release. This means that Ca^{2+} will diffuse only a few microns before being bound or removed, thereby limiting trapping of Ca^{2+} by spines.

We next considered movement of IP_3, a second messenger that also is involved in regulation of synaptic efficacy in PC dendrites (Khodakhah and Armstrong, 1997; Finch and Augustine, 1998;Miyata et al., 2000;Doi et al., 2005). We uncaged IP_3 focally and monitored its diffusion indirectly, by tracking the subsequent release of Ca^{2+} from intracellular stores. Given the above indications that Ca^{2+} diffuses very little, we expected that any time-dependent fluorescence changes would arise from movement of IP_3 rather than Ca^{2+}. Local uncaging of IP_3 released Ca^{2+} locally (Fig. 9A), as previously reported (Finch and Augustine, 1998). The IP_3-induced rise in $[Ca2+]_i$ occurred after a delay of a few ms and reached a peak level that was sustained for a few hundred ms before subsiding (Fig. 9B). Unlike the $[Ca^{2+}]_i$ rise produced by uncaging Ca^{2+} directly, this $[Ca^{2+}]_i$ signal spread over time, so that the spatial profiles measured at different times crossed over each other (Fig. 9C). This spread of the IP_3-induced Ca^{2+} signal in spiny dendrites could be described by an anomalous diffusion process, with a very steep slope on logarithmic plots (Fig. 9D, filled symbols). In smooth dendrites, these signals also exhibited anomalous diffusion behavior, though the slope of logarithmic plots was much less steep (Fig. 9D, open symbols). There was a significant difference ($p<0.01$, Mann-Whitney non-parametric test) in the mean values of d_w (Fig. 9E) determined for spiny dendrites (10.9 ±1.7 S.E.M.; n = 4) and for smooth dendrites (4.5±0.4, n = 6). The fact that d_w in smooth dendrites was substantially greater than 2, in the absence of spines, suggests that diffusion of IP_3 also is affected by other factors. Prime candidates for such factors are intracellular binding and degradation, which can cause anomalous diffusion (Saxton, 1996) and are known to occur in the case of IP_3 (Pattni and Banting, 2004). In summary, our analyses suggest that diffusional spread of IP_3 in dendrites is anomalous and that this arises from 2 sources: IP_3 metabolism and spine trapping.

DISCUSSION

Using a combination of optical experiments and computer simulations, we have determined that dendritic spines act as traps to produce anomalous diffusion of molecules along dendrites of cerebellar PCs. Our results indicate that spines influence dendritic structure in a way that limits the spread of intracellular chemical signals. Spines trap not only the inert volume marker FD, but also the second messenger IP_3. Trapping of Ca2+ is limited, because these ions are rapidly sequestered or otherwise removed from the PC.

We considered several alternative explanations for the observed power-law time course of fluorescence spatial variance in spiny dendrites. Our simulations showed that the experimentally measured rates of FD diffusion in PC dendrites could not be attributed to the branching of these dendrites, their finite length, or to changes in dendritic diameter. In addition, our experimental measurements showed that FD molecules were not bleached significantly over the time of the measurements and, in any case, simulations established that bleaching could not account for the observed time-dependent slowing of D_{app}. Instead, both the simulations and the experiments indicated that the presence of spines causes a fundamental change in the nature of the diffusion of molecules along dendrites. Simulations also indicated that this change is not simply due to an increase in the relative volume of the spines. Instead,

NIH-PA Author Manuscript

NIH-PA Author Manuscript

NIH-PA Author Manuscript

both simulations and experiments point to the conclusion that dendritic spines trap molecules, leading to anomalous diffusion in PCs. Further work will be needed to determine whether spine trapping occurs in other neuron types.

Anomalous diffusion is a breakdown of the laws of mass action (Schnell and Turner, 2004). As opposed to normal diffusion, in which the movement of molecules is not correlated with their previous position, during anomalous diffusion molecules are spatially and temporally correlated (ben-Avraham and Havlin, 2005). This spatio-temporal correlations reflect a fundamentally different behavior which, for example, affects spread of molecules within membranes (Saxton and Jacobson, 1997) and the generation of biochemical reactions in the cytoplasm (Schnell and Turner, 2004). Anomalous diffusion also is distinct from aggregation mechanisms, for example those involved in concentrating neurotransmitter receptors at postsynaptic membranes (Poo and Young, 1990;Triller and Choquet 2005). Such aggregation mechanisms involve the near-permanent trapping of molecules, while anomalous diffusion causes molecular movement to be slowed but not stopped.

Although the largest contribution to anomalous diffusion in PCs is from spines, there is a small amount observed in smooth dendrites. This low amount of anomalous diffusion could be due to the presence of intracellular organelles or crowding by macromolecules (Saxton, 1995; Schnell and Turner, 2004). This apparently varies among cell types, because diffusion in smooth dendrites of cerebellar interneurons is normal (Soler-Llavina and Sabatini, 2006). Such differences may reflect differences in the intracellular composition of interneurons and PCs (Lafarga et al., 1991).

Molecules can transit from anomalous to normal diffusion, with anomalous diffusion typically observed at earlier times (Saxton and Jacobson, 1997;Ritchie et al., 2003). In the case of PCs, the prevalence of anomalous diffusion, for at least 1 s, is due to short-range correlations caused by diffusible molecules being trapped in spines. Our experimental results suggest that anomalous diffusion will affect molecules with a cytoplasmic half-life of several hundred milliseconds or longer. Binding to intracellular constituents and/or intracellular degradation can further influence the value of the anomalous exponent, increasing the exponent - as in the case of IP_3 and possibly any intracellular signal that is not rapidly removed from the cytoplasm - or preventing anomalous diffusion by avoiding spine trapping, as in the case of Ca^{2+}. Thus, spines and intracellular reactions can combine to exert strong control over the movement of physiologically important chemical signals.

Until now, characterization of diffusion has relied almost exclusively on measurements of diffusion coefficients (e. g., Fukatsu et al., 2004;Schmidt et al., 2005). Diffusion coefficients typically are calculated by comparing the relative spread of a fluorescent molecule over two time points (Fritzsch, 1993), or by measuring the time constant of recovery after photobleaching (Axelrod et al., 1976;Fukano et al., 2004). Our analysis indicates that such apparent diffusion coefficients may not be constant, but instead can vary over time, even for an inert molecule such as FD. Our observations of differences in diffusional behavior within two different types of dendrites in the same cell also indicate that diffusion coefficients can exhibit regional differences within single cells. For these reasons, our analysis indicates that measuring the anomalous exponent may be the most reliable way to characterize diffusion, particularly in spiny dendrites.

Trapping of molecules by spines can exert at least two types of effects that could be important for dendritic function. First, spines will have a strong influence on how far and how fast locally produced molecules will travel within dendrites. Over a time scale of 1 s, a molecule with a D_o of 2 μm^2/ms (on the high end for a physiologically relevant molecule; Hille, 2001), would diffuse about 60 μm. Thus, as long as molecules remain in the cytosol, their movement could

NIH-PA Author Manuscript

NIH-PA Author Manuscript

NIH-PA Author Manuscript

be dominated by an anomalous diffusion process over distances as long as entire dendrite branches. Second, anomalous diffusion reflects an increase in the spatial and temporal correlation of diffusing molecules (Schnell and Turner, 2004) which would be expected to promote activation of biochemical networks by intracellular signals trapped in spines. Dynamic changes in spine volume, for example as occurs during long-term synaptic plasticity (Lang et al., 2004;Matsuzaki et al., 2004;Zhou et al., 2004), have been proposed to regulate synaptic efficacy by controlling AMPA receptor levels in the spine head (Matsuzaki et al., 2004). Our results suggest that alterations in spine structure could also influence spine trapping and dendritic diffusion, thereby affecting the interaction of signaling molecules within spines. This could contribute to "synaptic tagging", the selective trapping of dendritic molecules by active spines that may be required for long-term plasticity (Frey and Morris, 1997).

Many experimental studies have shown that the spine neck can serve as a diffusion barrier to slow spread from the spine head into the dendritic shaft, leading to the idea that spines can serve as biochemically isolated compartments (Svoboda et al., 1996;Majewska et al., 2000;Nimchinsky et al., 2002;Goldberg and Yuste, 2005;Noguchi et al., 2005). Our results complement this work by revealing a novel function for spines in PCs: these spines can serve as diffusion traps, thereby generating anomalous diffusion of molecules along dendrites and within spines.

EXPERIMENTAL PROCEDURES

Green's Function Monte Carlo simulations

Simulating diffusion—We modeled diffusion within a dendrite consisting of cylindrical compartments. In each compartment we implemented an algorithm to solve the general form of the diffusion equation:

$$\frac{\partial C}{\partial t} = D_0 Laplacian\,(C) \qquad 5$$

where C is concentration and D_o is the diffusion coefficient (Crank, 1975). For a cylinder the Laplacian has this form:

$$\frac{\partial C}{\partial t} = D_0 \frac{\partial^2 C}{\partial r^2} + \frac{D_0}{r}\frac{\partial C}{\partial r} + \frac{D_0}{r^2}\frac{\partial^2 C}{\partial \theta^2} + D_0 \frac{\partial^2 C}{\partial z^2} \qquad 6$$

where r, θ, and z are the radial, angular, and axial positions along the main axis, respectively. Two major strategies exist to solve this equation numerically: numerical integration and Monte Carlo (MC) simulations. Numerical integration tracks continuous concentration changes in all the points of the lattice (De Schutter, 1998). MC simulations of diffusion, on the other hand, typically require tracking the movement of individual molecules that are randomly walking within the volume (Stiles and Bartol, 2000).

Our experiments measuring diffusion in dendrites involved photolysis of caged compounds in dendritic compartments 1–5μm in length and less than 4 μm in diameter. With concentrations ranging from 0.1–100 mM, the number of molecules released is in the order of 10^7–10^9, making the simulation of such experiments computationally demanding. The structure of dendrites also spans several spatial scales, from dendritic spines, with volumes under 1 μm^3, to dendritic segments with diameters between 1–8 μm (Fiala and Harris, 1999). These properties made neither method attractive for our diffusion simulations.

In order to solve the diffusion equation under the complex boundary conditions and spatial scales in dendritic trees, we implemented an approach that uses a Green's Function Monte

NIH-PA Author Manuscript

NIH-PA Author Manuscript

NIH-PA Author Manuscript

Carlo method (GFMC; Bormann, 2001). The method consists in converting the initial condition into *walkers*, each of which represents a finite, discrete number of molecules that occupy a discrete position $\mathbf{r} = (l_r, l_\theta, l_z)$ on a cylindrical lattice. The number of molecules per walker, and the spatial resolution of the lattice are selected as trade-offs between accuracy and efficiency of the simulation. The setup consists in selecting the number of molecules per walker (M_w, usually 100) and the spatial resolution along the axis of the dendrite (d_z, usually 0.05 μm). The molecules are fully defined by their diffusion coefficient in artificial intracellular solution (D_{free}). We then defined dendritic structure (see below) and initial conditions, which depend on the initial concentration (I_m) and volume it occupies (V in μm^3).

The initial number of molecules is given by:

$$T_m = \mathrm{round}(1e^{-18} * I_m * V * N_A), \tag{7}$$

where $1e^{-18}$ converts from mol/m^3 to $mol/\mu m^3$, and N_A is the Avogadro number. The total number of walkers is given by:

$$N_w = |T_m / M_w|_R , \tag{8}$$

where the $|\,|_R$ operator randomly rounds the number of walkers up or down using probabilities given by the fractional part.

The algorithm treats every walker as a single unit that performs a random walk over the lattice. The movement of each individual walker at each time step Δt is controlled, independently for each degree of freedom w, by a step size $\Delta w(\mathbf{r})$, and by a binomial distribution with probabilities $p_{w,+/-}(\mathbf{r})$ that determines in which direction the walker takes a step. The second and third term of eq. 6 suggest a dependence of $p_{r,+/-}(\mathbf{r})$ and $\Delta\theta(\mathbf{r})$ on l_r, respectively. To effectively solve the diffusion equation two steps have to be drawn per iteration. Therefore the spatial and temporal steps are determined by:

$$\begin{aligned} \Delta t &= d_z^2 / (4 * D), \\ \Delta r^2 &= \Delta z^2 = d_Z^2, \\ \Delta\theta^2(I_r > 0) &= \Delta r^2 / I_r^2. \end{aligned} \tag{9}$$

The directional probabilities for each dimension are given by:

$$\begin{aligned} p_{r,+/-} &= \frac{1}{2}(1 + / - 1 / I_r), \\ p_{\theta,+/-} &= p_{z,+/-} = \frac{1}{2}. \end{aligned} \tag{10}$$

In the limit of $\Delta t \to 0$, with all other parameters scaling accordingly, this random walk mechanism provides a good approximation to a Wiener process, which in turn provides a fundamental solution to the diffusion process in the absence of drift. By applying this fundamental solution to all walkers individually, we solve the diffusion equation for any combination of initial conditions.

Boundary conditions—Boundary conditions were checked and handled on even time steps. There are three types of boundaries: Walls, serial concatenations, and spines perpendicularly attached to the surface of a cylinder. The walls surrounding each individual compartment are treated as reflecting surfaces:

NIH-PA Author Manuscript

NIH-PA Author Manuscript

NIH-PA Author Manuscript

$$p_{r,+}(I_r = 0) = 1,\ p_{r,-}(I_r = R) = 1$$
$$p_{z,+}(I_z = 0) = 1,\ p_{z,-}(I_z = L) = 1, \quad (11)$$

with R and L the radius and length of the compartment, respectively. Since each cylinder has its own local coordinate system, geometric conversions were implemented to allow the transition of walkers between serially and perpendicularly (spines) concatenated compartments. The spine and dendrite have to overlap by the minimal intersection of the two cylinders in which the entire perimeter of the spine is within the dendrite. A random number determines if a walker in this overlapping region is transferred from one compartment to the other (Bormann, 2001).

Implementation—The algorithm was implemented within GENESIS (Bower and Beeman, 1995). The simulations recorded the total concentration at 0.05 μm thick longitudinal sections along the axis of the dendrite, unless otherwise specified. We ran multiple simulations (8, 16, or 32) with different initializations of the random number generator to investigate the variability in concentration on different structures. The program was implemented on Linux desktops and then ported to parallel architectures at the San Diego Super Computer Center. Analysis of the data was done using Matlab (Natick, MA).

Calculating diffusion coefficients

We assumed a one-dimensional diffusion process along the axis of the dendrite described by:

$$\left\langle x^2 \right\rangle = 2D_0 t \quad (12)$$

where $<x^2>$ is the variance at each time point, D_o the diffusion coefficient, and t time. The variance of the distribution was calculated in the following way:

$$\left\langle x^2 \right\rangle = \sum_x (x - r_m(t))^2 C_n(x, t) \quad (13)$$

where $r_m(t)$ is the mean (or centroid) at each time point (eq. 13a), $C_n(x,t)$ the spatial concentration profile, proportional to the fluorescence, normalized to its area (eq. 13b). Before calculating the variance each frame was background corrected, and the raw fluorescence along the entire width of the dendrite ($F(x,t)$) was integrated every 1 micron along the axis of the dendrite. We then convolved the resulting fluorescent profile with a Gaussian of 2 μm standard deviation ($E(x)$, eq. 13c).

$$r_m = \frac{\int_x x C_n(x, t)\, dx}{\int_x C_n(x, t)\, dx} \quad (13a)$$

$$C_n(x, t) = \frac{\frac{\Delta G(x, t)}{G_0(x)}}{\int_x \frac{\Delta G(x, t)}{G_0(x)}\, dx} \quad (13b)$$

$$G(x, t) = \int_\tau E(x, \tau) F(x, t - \tau)\, d\tau \quad (13c)$$

The level of fluorescence before the stimulus (G_o) was calculated using at least 10 frames of the Texas Red fluorescence. We then calculated D_{app} using eq. 14:

NIH-PA Author Manuscript

NIH-PA Author Manuscript

NIH-PA Author Manuscript

$$D_{app}(t) = \frac{\langle x^2 \rangle - \langle x^2 \rangle_0}{2t} \quad 14$$

where $\langle x^2 \rangle_o$ is the variance of the initial condition.

The accuracy of our modeling approximation was validated by integrating the diffusion equation for several cases, which yielded results very similar to our numerical models (Bormann et al., 2001). We also performed several simulations with different time steps from 1 to 3 μs; these resulted in spatial steps of 0.01 to 0.05 μm, but had little effect on the results. The minimum cylindrical structure was 0.1 μm in diameter and 0.1 μm in length.

Experimental procedures

Sagittal slices from the cerebellar vermis were prepared from mice 12–17 days old (Finch and Augustine, 1998), following procedures approved by the Animal Care and Use Committee of the Duke University Medical Center. The extracellular solution was composed of (in mM): NaCl, 125; KCl, 2.5; $CaCl_2$, 2; MgCl, 1.3; NaH_2PO_4, 1.25; $NaHCO_3$, 26; D-glucose, 20. The free radical scavenger trolox-C (0.1 mM) was added to the extracellular solution to reduce phototoxicity.

Whole cell patch clamp recordings were made from the somata of PCs (Finch and Augustine, 1998). The intracellular recording solution was composed of (in mM): potassium gluconate, 130; NaCl, 2; Na_2ATP, 4; Na-GTP, 0.4; $MgCl_2$, 4; Hepes (pH 7.2), 30 mM; EGTA, 0.5. Caged flourescein dextran (FD; 3 kD molecular mass; 2–5 mM) and Texas Red dextran (10 kD, 0.5 mM) were added to these solutions as needed. For analysis of calcium diffusion, we reanalyzed images obtained previously (Miyata et al., 2000). For those experiments, the patching pipette was filled with caged calcium (DMNPE-4; Ellis-Davies, 1998) and a high affinity calcium indicator (Oregon Green BAPTA-1, Molecular Probes). Similarly, IP_3 diffusion data were extracted from images described in Finch and Augustine (1998), using caged IP_3 (Walker et al., 1989) and the same calcium indicator. Fluorescence images were acquired using a high-speed confocal microscope (Noran Odyssey, Madison, WI) at 120 frames per second. Caged compounds were photolyzed by brief flashes (3–5 ms duration) from a shuttered UV laser (Coherent Innova 305), as described in Wang & Augustine (1995). The total amount of UV energy was 3–10 μJ. Images were analyzed with routines written in Matlab. All pseudocolor images were thresholded at 20% $\Delta F/F_o$, which was approximately twice the background noise level.

Supplementary Material

Refer to Web version on PubMed Central for supplementary material.

Acknowledgements

Supported by HFSP RGP0074/200, NIH NS-34045 and GM65473, NPACI, and FWO (Belgium). We thank A. Lin and E. Monson for helpful comments and K. Berglund, Q. Cheng, S. Raghavachari, K. Tanaka, and R. Yasuda for careful reading of an earlier version of this paper.

References

Allbritton NL, Meyer T, Stryer L. Range of messenger action of calcium ion and inositol 1,4,5-trisphosphate. Science 1992;258:1812–1815. [PubMed: 1465619]

Augustine GJ, Santamaria F, Tanaka K. Local calcium signaling in neurons. Neuron 2003;40:331–346. [PubMed: 14556712]

Axelrod D, Koppel DE, Schlessinger J, Elson E, Webb WW. Mobility measurement by analysis of fluorescence photobleaching recovery kinetics. Biophys J 1976;16:1055–1069. [PubMed: 786399]

NIH-PA Author Manuscript

NIH-PA Author Manuscript

NIH-PA Author Manuscript

ben-Avraham, D.; Havlin, S. Diffusion and reactions in fractals and disordered systems. Cambridge; Cambridge University Press: 2000.

Bird GS, Aziz O, Lievremont JP, Wedel BJ, Trebak M, Vazquez G, Putney JW Jr. Mechanisms of phospholipase C-regulated calcium entry. Curr Mol Med 2004;4:291–301. [PubMed: 15101686]

Bormann, G.; Brosens, F.; De Schutter, E. Diffusion. In: Bower, JM.; Bolouri, H., editors. Computational Modeling of Genetic and Biochemical Networks. MIT press; 2001.

Bower, JM.; Beeman, D. The book of GENESIS. New York: Springer-Verlag; 1995.

Crank, J. The mathematics of diffusion. Oxford: Clarendon Press; 1975.

De Schutter, E.; Smolen, P. Calcium dynamics in large neuronal models. In: Koch, C.; Segev, I., editors. Methods in neruonal modeling. Cambridge; MIT press: 1998.

Doi T, Kuroda S, Michikawa T, Kawato M. Inositol 1,4,5-trisphosphate-dependent Ca2+ threshold dynamics detect spike timing in cerebellar Purkinje cells. J Neurosci 2005;25:950–961. [PubMed: 15673676]

Edgerton JR, Reinhart PH. Distinct contributions of small and large conductance Ca^{2+}-activated K^{+} channels to rat Purkinje neuron function. J Physiol 2003;548:53–69. [PubMed: 12576503]

Ellis-Davies G. Synthesis of Photolabile EGTA Derivatives. Tetrahedron Letters 1998;39:953–956.

Fiala, JC.; Harris, KM. Dendrite structure. Stuart, Dendrites G.; Nelson, S.; Hausser, M., editors. Oxford: Oxford University Press; 1999.

Fierro L, DiPolo R, Llano II. Intracellular calcium clearance in Purkinje cell somata from rat cerebellar slices. J Physiol (Lond) 1998;510:499–512. [PubMed: 9705999]

Fierro L, Llano II. High endogenous calcium buffering in Purkinje cells from rat cerebellar slices. J Physiol (Lond) 1996;496:617–625. [PubMed: 8930830]

Finch EA, Augustine GJ. Local calcium signalling by inositol-1,4,5-trisphosphate in Purkinje cell dendrites. Nature 1998;396:753–756. [PubMed: 9874372]

Frey U, Morris RG. Synaptic tagging and long-term potentiation. Nature 1997;385:533–536. [PubMed: 9020359]

Fritzsch B. Fast axonal diffusion of 3000 molecular weight dextran amines. J Neurosci Methods 1993;50:95–103. [PubMed: 7506342]

Fukano T, Hama H, Miyawaki A. Similar diffusibility of membrane proteins across the axon-soma and dendrite-soma boundaries revealed by a novel FRAP technique. J Struct Biol 2004;147:12–18. [PubMed: 15109601]

Fukatsu K, Bannai H, Zhang S, Nakamura H, Inoue T, Mikoshiba K. Lateral diffusion of inositol 1,4,5-trisphosphate receptor type 1 is regulated by actin filaments and 4.1N in neuronal dendrites. J Biol Chem 2004;279:48976–48982. [PubMed: 15364918]

Goldberg JH, Yuste R. Space matters: local and global dendritic Ca2+ compartmentalization in cortical interneurons. Trends Neurosci 2005;28:158–167. [PubMed: 15749170]

Gundappa-Sulur G, De Schutter E, Bower JM. Ascending granule cell axon: an important component of cerebellar cortical circuitry. J Comp Neurol 1999;408:580–596. [PubMed: 10340507]

Harris KM, Stevens JK. Dendritic spines of rat cerebellar Purkinje cells: serial electron microscopy with reference to their biophysical characteristics. J Neurosci 1988;8:4455–4469. [PubMed: 3199186]

Harvey RJ, Napper RM. Quantitative studies on the mammalian cerebellum. Prog Neurobiol 1991;36:437–463. [PubMed: 1947173]

Hartmann J, Konnerth A. Determinats of postsynaptic Ca2+ signaling in Purkinje neurons. Cell Calcium 2005;37(5):459–466. [PubMed: 15820394]

Hille, B. Ion channels of excitable membranes. Sunderland: Sinauer Associates; 2001.

Holthoff K, Tsay D, Yuste R. Calcium dynamics of spines depend on their dendritic location. Neuron 2002;33:425–437. [PubMed: 11832229]

Klafter J, Sokolov IM. Anomalous diffusion spreads its wings. Physics World 2005;18:29–32.

Konnerth A, Dreessen J, Augustine GJ. Brief dendritic calcium signals initiate long-lasting synaptic depression in cerebellar Purkinje cells. Proc Natl Acad Sci U S A 1992;89:7051–7055. [PubMed: 1323125]

NIH-PA Author Manuscript

NIH-PA Author Manuscript

NIH-PA Author Manuscript

Lafarga M, Berciano MT, Garcia-Segura LM. Freeze-fracture organization of chromatin and cytoplasm in neurons and astroglia of rat cerebellar cortex. Journal of Neurocytology 1991;20:533–551. [PubMed: 1919602]

Lang C, Barco A, Zablow L, Kandel ER, Siegelbaum SA, Zakharenko SS. Transient expansion of synaptically connected dendritic spines upon induction of hippocampal long-term potentiation. Proc Natl Acad Sci U S A 2004;101:16665–16670. [PubMed: 15542587]

Maeda H, Ellis-Davies GC, Ito K, Miyashita Y, Kasai H. Supralinear Ca^{2+} signaling by cooperative and mobile Ca^{2+} buffering in Purkinje neurons. Neuron 1999;24:989–1002. [PubMed: 10624961]

Majewska A, Tashiro A, Yuste R. Regulation of spine calcium dynamics by rapid spine motility. J Neursci 2000;20 (22):8262–8268.

Martone ME, Zhang Y, Simpliciano VM, Carragher BO, Ellisman MH. Three-dimensional visualization of the smooth endoplasmic reticulum in Purkinje cell dendrites. J Neurosci 1993;13:4636–4646. [PubMed: 8229189]

Matsuzaki M, Honkura N, Ellis-Davies GC, Kasai H. Structural basis of long-term potentiation in single dendritic spines. Nature 2004;429:761–766. [PubMed: 15190253]

Michailova A, DelPrincipe F, Egger M, Niggli E. Spatiotemporal features of Ca2+ bufferering and diffusion in atrial cardiac myocytes with inhibited sarcoplasmic reticulum. Biophys J 2002;83(6): 3134–51. [PubMed: 12496084]

Miyata M, Finch EA, Khiroug L, Hashimoto K, Hayasaka S, Oda SI, Inouye M, Takagishi Y, Augustine GJ, Kano M. Local calcium release in dendritic spines required for long-term synaptic depression. Neuron 2000;28:233–244. [PubMed: 11086997]

Nakamura T, Lasser-Ross N, Nakamura K, Ross WN. Spatial segregation and interaction of calcium signalling mechanisms in rat hippocampal CA1 pyramidal neurons. J Physiol 2002;543:465–480. [PubMed: 12205182]

Nimchinsky EA, Sabatini BL, Svoboda K. Structure and function of dendritic spines. Annu Rev Physiol 2002;64:313–353. [PubMed: 11826272]

Neher E, Augustine GJ. Calcium gradients and buffers in bovine chromaffin cells. J Physiol 1992;450:273–301. [PubMed: 1331424]

Ngo-Anh TJ, Bloodgood BL, Lin M, Sabatini BL, Maylie J, Adelman JP. SK channels and NMDA receptors form a Ca2+-mediated feedback loop in dendritic spines. Nat Neurosci 2005;8:642–649. [PubMed: 15852011]

Noguchi J, Matsuzaki M, Ellis-Davies GC, Kasai H. Spine-neck geometry determines NMDA receptor-dependent Ca^{2+} signaling in dendrites. Neuron 2005;46:609–622. [PubMed: 15944129]

Palay; Chan-Palay. Cerebellax cortex. New York: Springer-Verlag; 1974.

Pattni K, Banting G. Ins(1,4,5)P3 metabolism and the family of IP3-3Kinases. Cell Signal 2004;16(6): 643–54. [PubMed: 15093605]

Poo MM, Young SH. Diffusional and electrokinetic redistribution at the synapse: a physicochemical basis of synaptic competition. J Neurobiol 1990;21:157–168. [PubMed: 2181061]

Ritchie K, Iino R, Fujiwara T, Murase K, Kusumi A. The fence and picket structure of the plasma membrane of live cells as revealed by single molecule techniques (Review). Mol Membr Biol 2003;20 (1):13–8. [PubMed: 12745919]

Sabatini BL, Maravall M, Svoboda K. Ca^{2+} signaling in dendritic spines. Curr Opin Neurobiol 2001;11:349–356. [PubMed: 11399434]

Saxton MJ. Anomalous diffusion due to obstacles: a Monte Carlo study. Biophys J 1994;66:394–401. [PubMed: 8161693]

Saxton MJ. Anomalous diffusion due to binding: a Monte Carlo study. Biophys J 1996;70:1250–1262. [PubMed: 8785281]

Saxton MJ, Jacobson K. Single-particle tracking: applications to membrane dynamics. Annu Rev Biophys Biomol Struct 1997;26:373–399. [PubMed: 9241424]

Schmidt H, Schwaller B, Eilers J. Calbindin D28k targets myo-inositol monophosphatase in spines and dendrites of cerebellar Purkinje neurons. Proc Natl Acad Sci USA 2005;102:5850–5855. [PubMed: 15809430]

NIH-PA Author Manuscript

NIH-PA Author Manuscript

NIH-PA Author Manuscript

Schmidt H, Stiefel KM, Racay P, Schwaller B, Eilers J. Mutational analysis of dendritic Ca^{2+} kinetics in rodent Purkinje cells: role of parvalbumin and calbindin D28k. J Physiol 2003;551:13–32. [PubMed: 12813159]

Schnell S, Turner TE. Reaction kinetics in intracellular environments with macromolecular crowding: simulations and rate laws. Prog Biophys Mol Biol 2004;85(2–3):235–60. [PubMed: 15142746]

Sepulveda MR, Hidalgo-Sanchez M, Mata AM. Localization of encoplasmic reticulum and plasma membrane Ca2+-ATPases in subcellular fractions and sections of pig cerebellum. Eur J Neurosci 2004;19(3):542–551. [PubMed: 14984405]

Sobczyk A, Scheuss V, Svoboda K. NMDA receptor subunit-dependent [Ca2+] signaling in individual hippocampal dendritic spines. J Neurosci 2005;25:6037–6046. [PubMed: 15987933]

Soler-Llavina GJ, Sabatini BL. Synapse-specific plasticity and compartmentalized signaling in cerebellar stellate cells. Nat Neurosci 2006;9:798–806. [PubMed: 16680164]

Stiles, J.; Bartol, TM. Monte Carlo methods for simulating realistic synaptic microphysiology using MCell. In: De Schutter, E., editor. Computatinal neuroscience. Boca Raton: CRC; 2000.

Svoboda K, Tank DW, Denk W. Direct measurement of coupling between dendritic spines and shafts. Science 1996;272 (5262):716–719. [PubMed: 8614831]

Triller A, Choquet D. Surface trafficking of receptors between synaptic and extrasynaptic membranes: and yet they do move! Trends Neurosci 2005;28:133–139. [PubMed: 15749166]

Walker JW, Feeney J, Trentham DR. Photolabile precursors of inositol phosphates. Preparation and properties of 1-(2-nitrophenyl)ethyl esters of myo-inositol 1,4,5-trisphosphate. Biochemistry 1989;28:3272–3280. [PubMed: 2787165]

Wang H, Storm DR. Calmodulin-regulated adenylyl cyclases: cross-talk and plasticity in the central nervous system. Mol Pharmacol 2003;63:463–468. [PubMed: 12606751]

Wang SS, Augustine GJ. Confocal imaging and local photolysis of caged compounds: dual probes of synaptic function. Neuron 1995;15:755–760. [PubMed: 7576625]

Weiss M, Elsner M, Kartberg F, Nilsson T. Anomalous subdiffusion is a measure for cytoplasmic crowding in living cells. Biophys J 2004;87:3518–3524. [PubMed: 15339818]

Womack MD, Chevez C, Khodakhah K. Calcium-activated potassium channels are selectively coupled to P/Q-type calcium channels in cerebellar Purkinje neurons. J Neurosci 2004;24:8818–8822. [PubMed: 15470147]

Yuste R, Majewska A, Cash SS, Denk W. Mechanisms of calcium influx into hippocampal spines: Heterogeneity among spines, coincidence detection by NMDA receptors, and optical quantal analysis. Journal of Neuroscience 1999;19:1976–1987. [PubMed: 10066251]

Zador A, Koch C. Linearized models of calcium dynamics: formal equivalence to the cable equation. Journal of Neuroscience 1994;14:4705–4715. [PubMed: 8046445]

Zhou Q, Homma KJ, Poo MM. Shrinkage of dendritic spines associated with long-term depression of hippocampal synapses. Neuron 2004;44:749–757. [PubMed: 15572107]

NIH-PA Author Manuscript
NIH-PA Author Manuscript
NIH-PA Author Manuscript

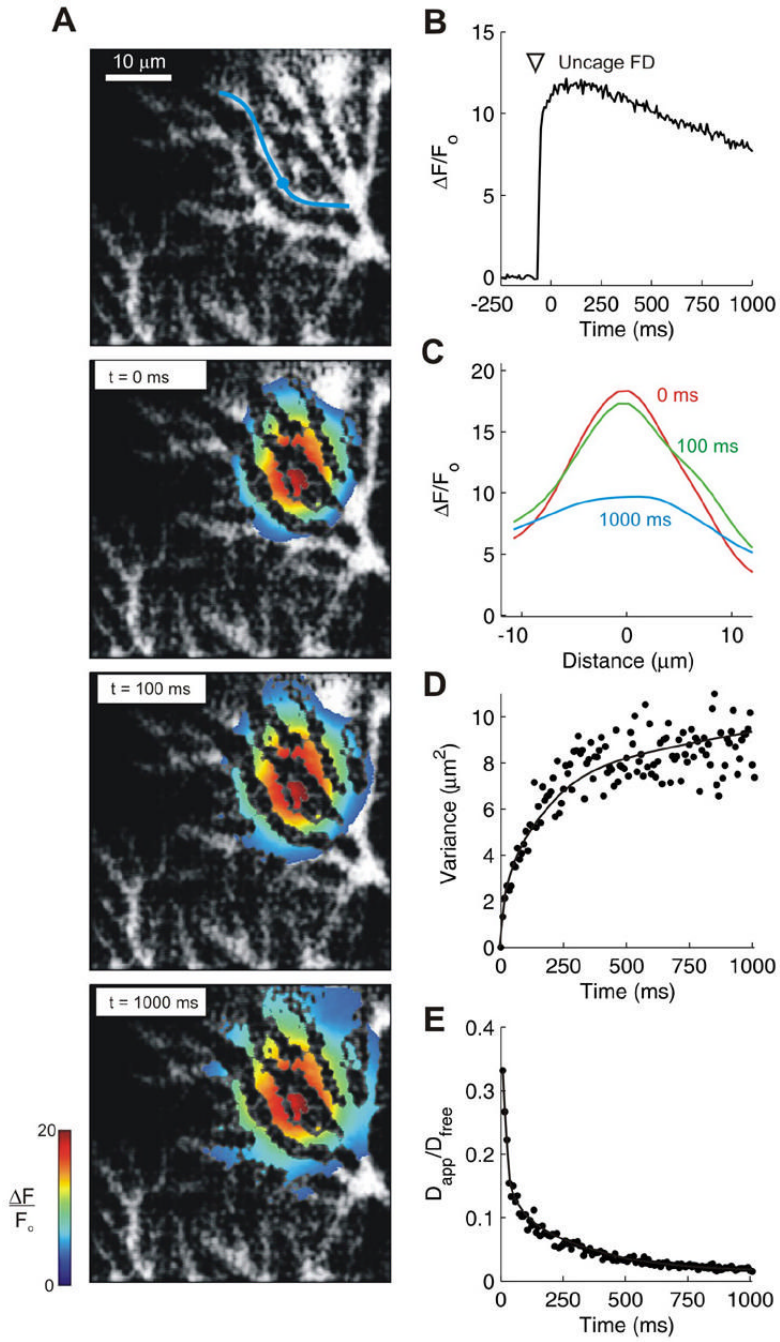

Figure 1.

Photolysis of caged FD in Purkinje cell spiny dendrites. (**A**) Confocal image of a spiny dendrite (top) and superimposed pseudocolor overlay of FD fluorescence at t = 0, 100 and 1000 ms after uncaging. The maximum of the pseudocolor scale corresponds to the peak value of FD fluorescence measured at t = 0. The blue line shows the pathway on which fluorescent profiles are tracked and the ● indicates the center of the uncaging spot. (**B**) Time course of fluorescence changes along the dendritic pathway marked in **A**. The ▽ indicates time of photolysis. (**C**) Spatial profiles of fluorescence changes along the same dendritic pathway, centered around the uncaging spot. The profiles were convolved with a 2 µm Gaussian function and were taken at 120 frames/s. (**D**) Spatial variance of $\Delta F/F_o$ over time, calculated from profiles such as those

shown in **C**. (**E**) D_{app} was calculated from spatial variance and was normalized by the diffusion coefficient for FD in free solution (D_{free}=0.08 μm^2/ms).

NIH-PA Author Manuscript
NIH-PA Author Manuscript
NIH-PA Author Manuscript

NIH-PA Author Manuscript

NIH-PA Author Manuscript

NIH-PA Author Manuscript

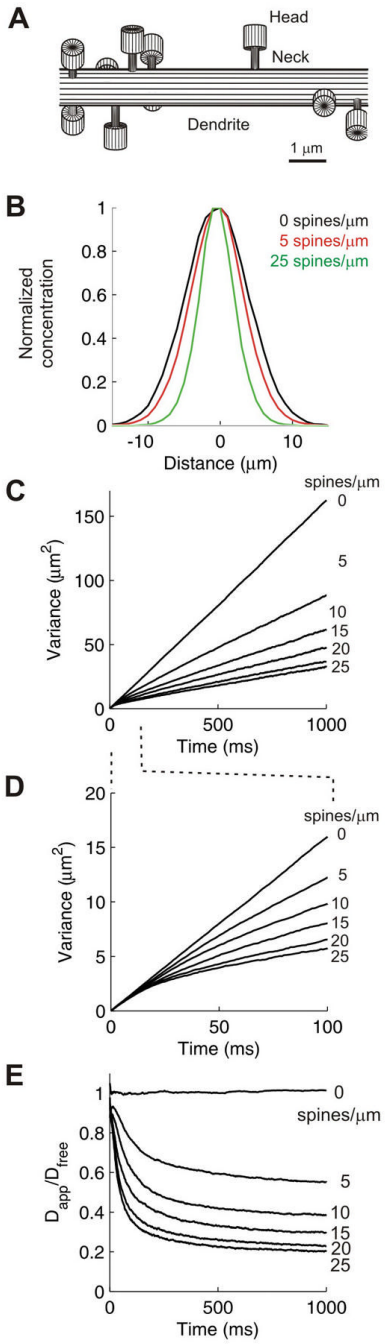

Figure 2.

Modeling diffusion in spiny dendrites. (**A**) Dendritic spines of different shapes were randomly attached to a smooth cylinder of diameter 1 μm and length 120 μm. (**B**) Normalized concentration profiles at t = 120 ms from simulations with the indicated densities of spines. (**C-D**) The spatial variance decreased non-linearly with increasing spine density (marked on each curve, spines/μm), particularly at early times (shown in **D**). (**E**) The non-linear time dependence of spatial variance resulted in strong sub-diffusion.

NIH-PA Author Manuscript

NIH-PA Author Manuscript

NIH-PA Author Manuscript

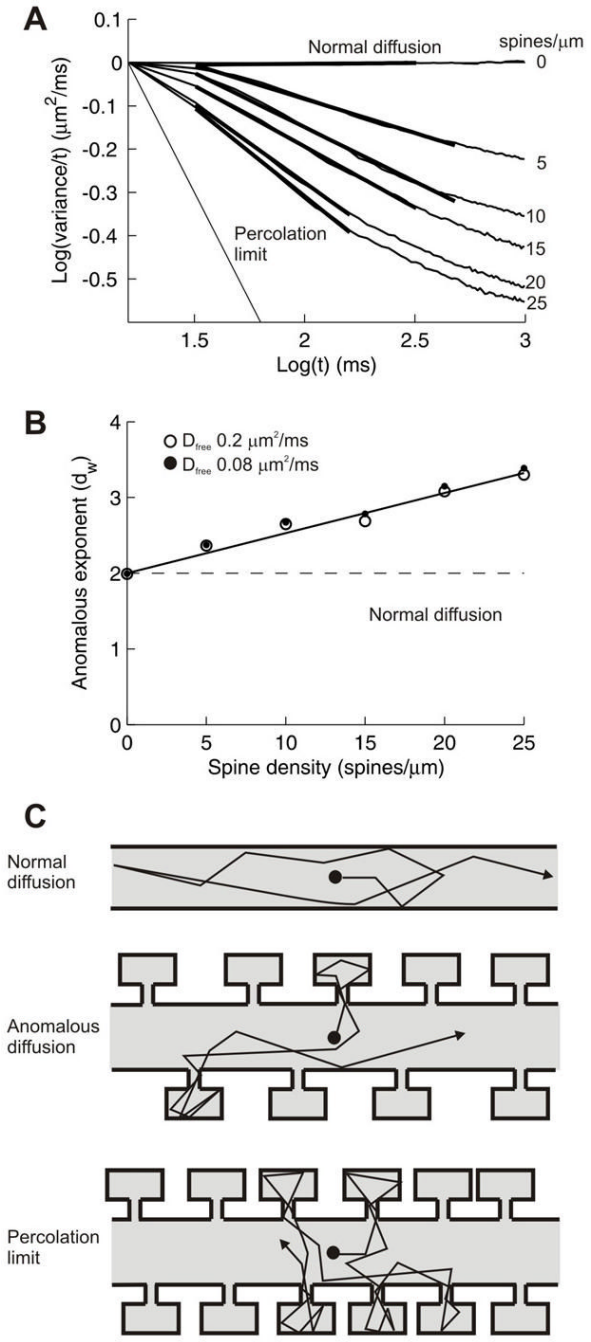

Figure 3.

Anomalous diffusion simulated in spiny dendrites. (**A**) The anomalous exponent (d_w) was extracted from the slope (thick lines) of plots of Log(variance/t) versus Log(t). In normal diffusion, m = 0 and $d_w = 2$; when m = −1 then $d_w \rightarrow$Inf and the percolation limit is reached. (**B**) Predicted values for d_w as a function of spine density, at two values of D_{free}. (**C**) In normal diffusion (top), there are no obstacles and molecules can diffuse freely along the dendritic axis. In the presence of dendritic spines (center), molecules enter spines and are trapped for some period of time before going back to the dendrite and diffusing along the dendritic axis. At a very high density of spines, the percolation limit is reached and molecules that escape from

NIH-PA Author Manuscript

NIH-PA Author Manuscript

NIH-PA Author Manuscript

one spine would enter another one and their axial diffusion is reduced so severely that D_{app} approaches zero.

NIH-PA Author Manuscript
NIH-PA Author Manuscript
NIH-PA Author Manuscript

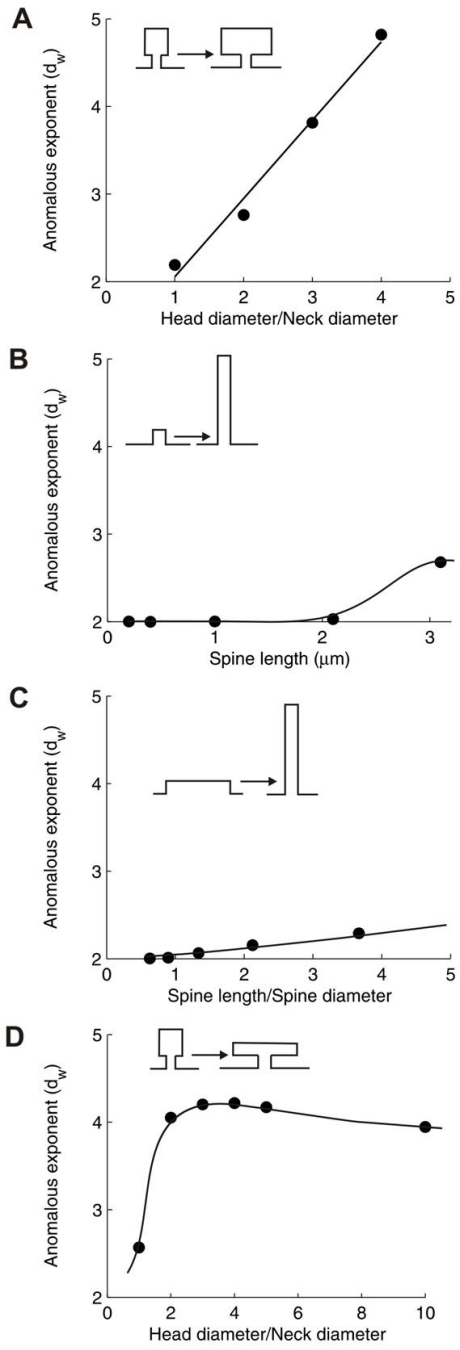

Figure 4.

Dendritic spine structure regulates anomalous diffusion. (**A**) Varying spine head volume, while keeping the spine neck parameters fixed, increased the anomalous exponent, d_w. (**B**) Varying spine length with a fixed spine neck diameter (0.3 μm, no spine head) had little effect on d_w. (**C**) Keeping the volume fixed while varying the spine diameter also had only a small effect. (**D**) The presence of a bottleneck between the spine head and neck increased the value of d_w considerably. The neck parameters were fixed and the spine head volume was constant, varying the head length and diameter. In all simulations we used the prototypical spine parameters: spine neck diameter 0.2 μm; neck length 0.6 μm; head diameter 0.6 μm; head length 0.6 μm, unless otherwise noted, at a fixed density of 15 spines/μm in a 1 μm diameter dendrite.

NIH-PA Author Manuscript
NIH-PA Author Manuscript
NIH-PA Author Manuscript

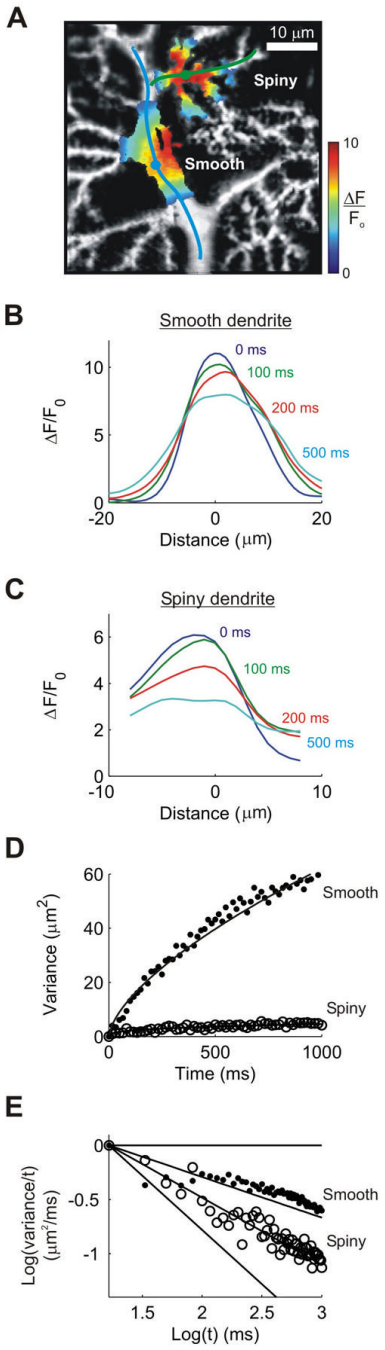

Figure 5.

Diffusion in smooth and spiny Purkinje cell dendrites. (**A**) Confocal image of a Purkinje cell dendrite showing smooth and spiny dendrites with superimposed pseudocolor overlay of FD fluorescence at t = 0 ms after two separate uncaging events. The maximum of the pseudocolor scale corresponds to the peak value of FD fluorescence measured at t = 0. The blue and green lines show the pathway on which fluorescent profiles were tracked and the ● indicates the center of the uncaging spot. (**B and C**) Spatial profiles of fluorescence along the indicated pathways in **A** for smooth (**B**) and spiny (**C**) dendrites. (**D**) Spatial variance of $\Delta F/F_o$ over time for the two paths indicated in **A**. (**E**) Logarithmic plots show anomalous diffusion in the spiny dendrite but practically normal diffusion in the smooth dendrite.

NIH-PA Author Manuscript

NIH-PA Author Manuscript

NIH-PA Author Manuscript

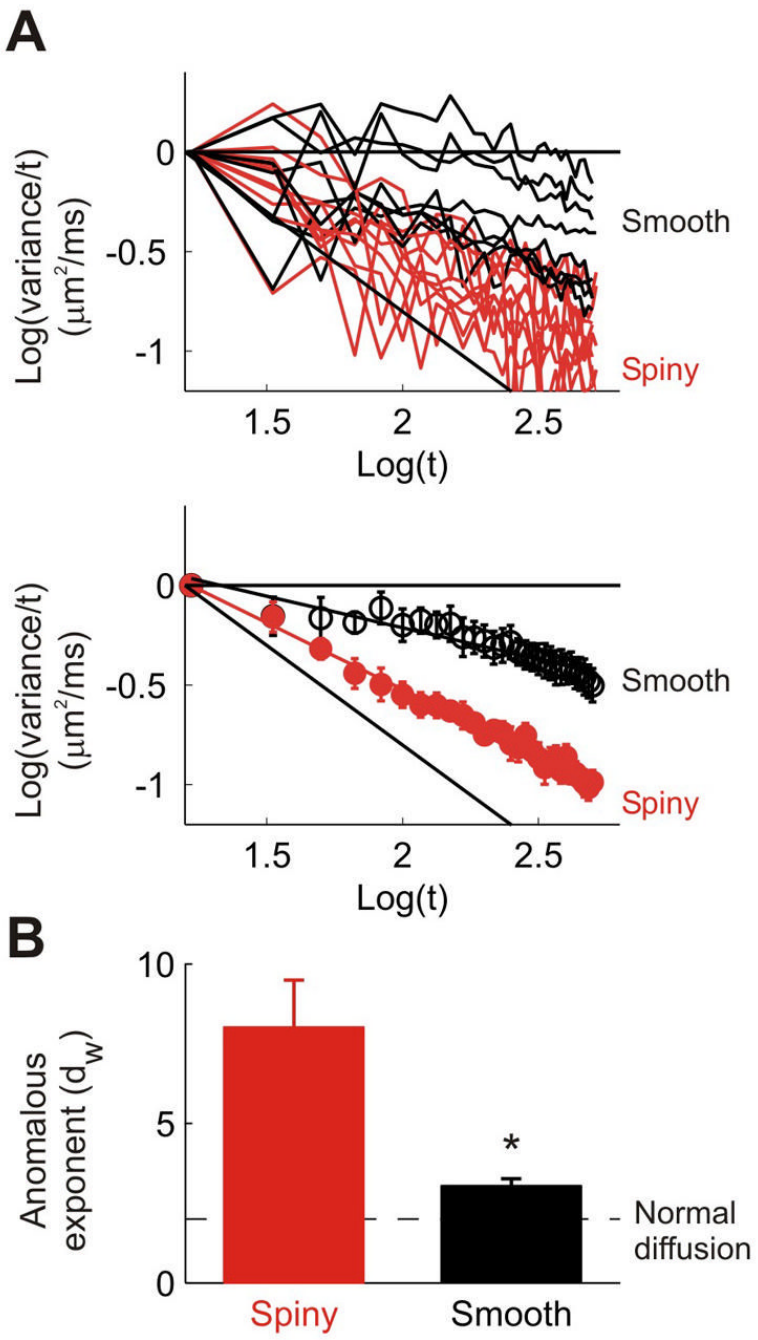

Figure 6.

Anomalous diffusion in living Purkinje cells. (**A**) Log(variance/t) vs. Log(t) for all the experiments (top) and average behavior (bottom) separated in smooth (black) and spiny dendrites (red). Each data point is the average of two replicates (bars are the S.E.M.). (**B**) Average values for the anomalous exponent determined in smooth and spiny dendrites (21 samples in 6 Purkinje cells, 11 in spiny- and 10 in smooth- dendrites). Asterisk indicates a statistically significant difference ($p<0.001$, Mann-Whitney test).

NIH-PA Author Manuscript
NIH-PA Author Manuscript
NIH-PA Author Manuscript

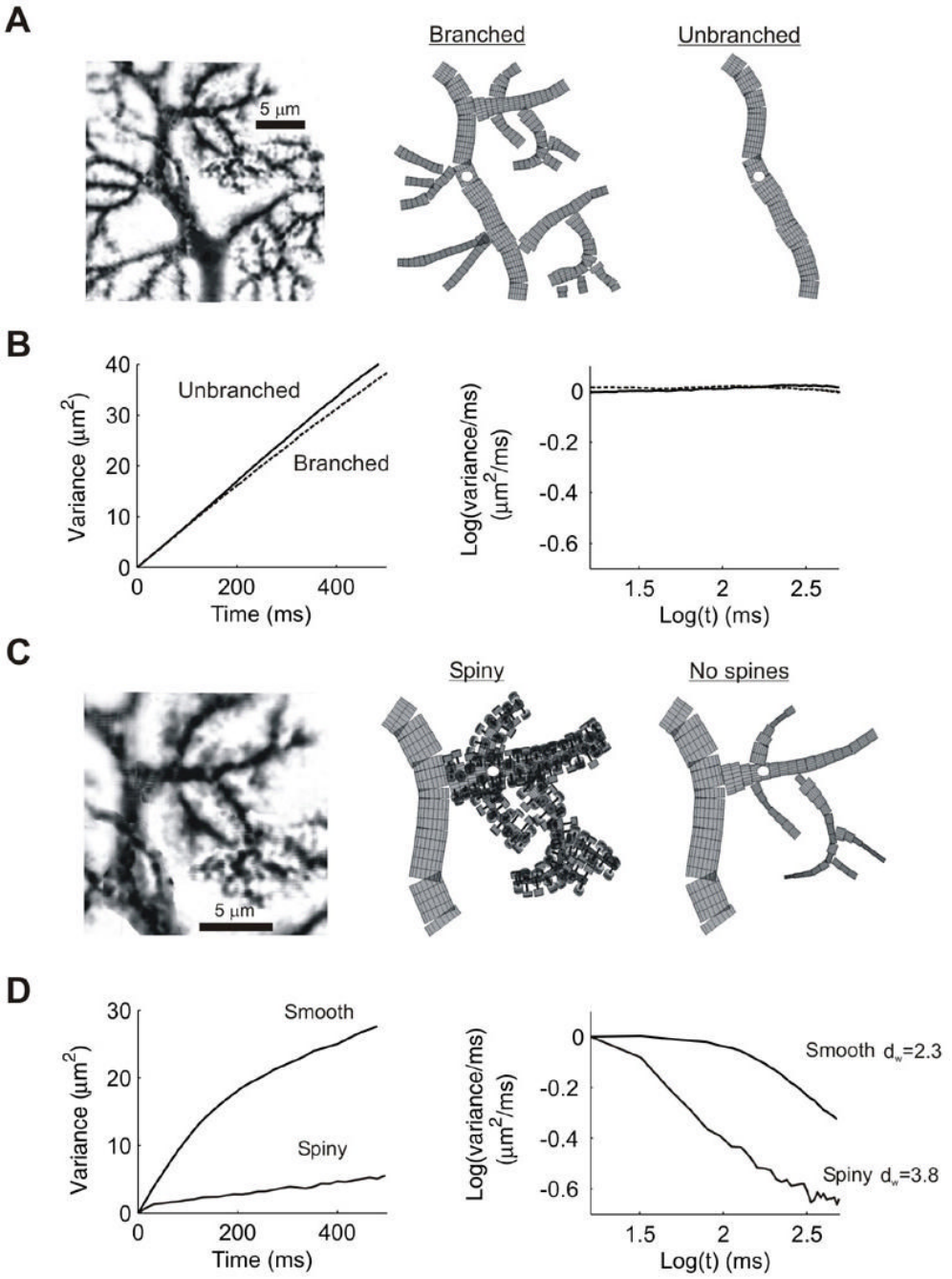

Figure 7.

Modeling diffusion in reconstructed dendritic architectures. (**A–B**) Diffusion in a thick smooth dendrite with (**A** branched) and without (**A** unbranched) branches. The plot of the variance against time (**B** left) and its logarithmic transform (**B** right) show no significant effect of branching on diffusion. (**C–D**) Variance against time on a branched dendrite covered with spines (**C** spiny) or smooth (**C** no spines), 11 spines/μm. The plot of the variance against time (**D** left) and its logarithmic transform (**D** right) show a strong influence of spines on diffusion. The data was analyzed with the same parameters used in the experiments. The white spots indicate site of initial release of molecules.

NIH-PA Author Manuscript
NIH-PA Author Manuscript
NIH-PA Author Manuscript

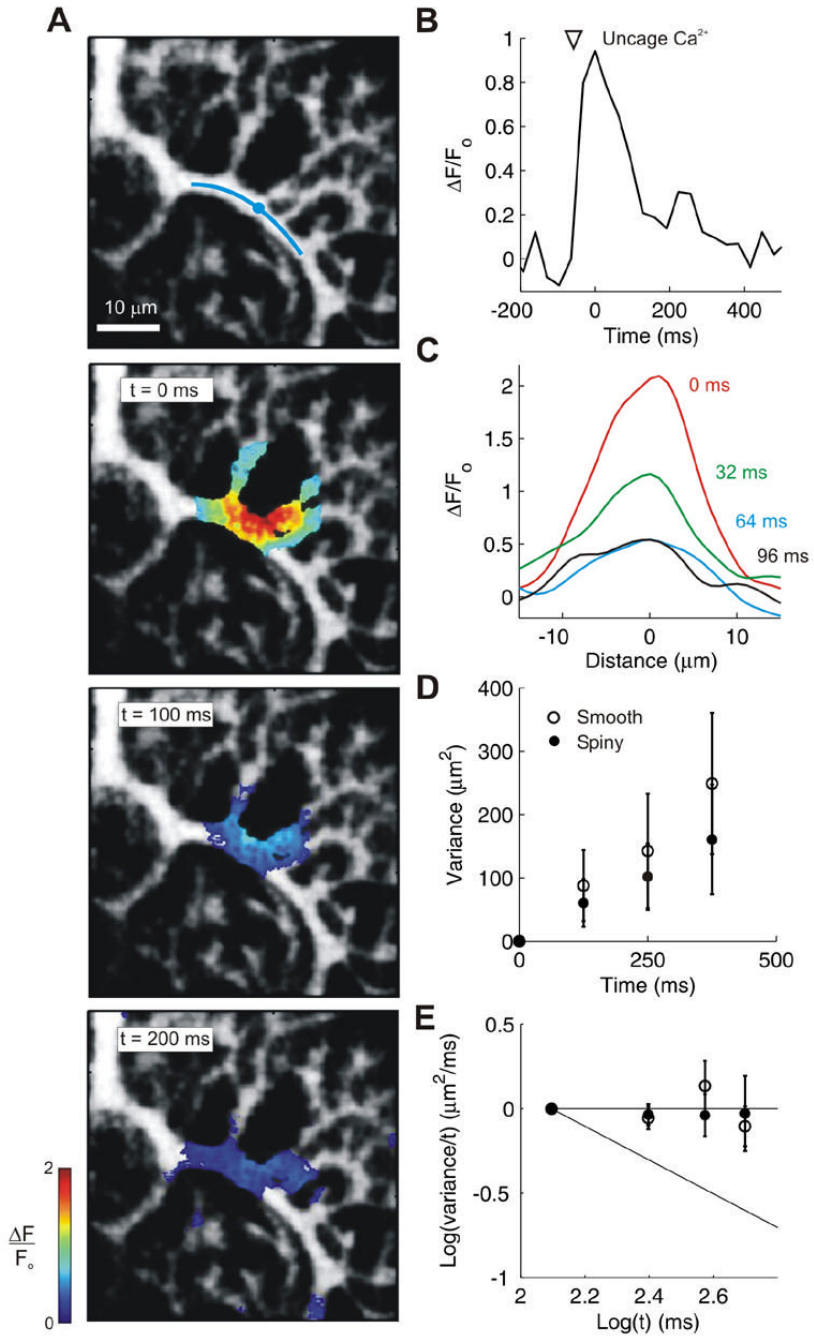

Figure 8.

Calcium diffusion in Purkinje cell dendrites is normal and not affected by dendritic structure. (**A**) Confocal images of a smooth dendrite and superimposed pseudocolor overlay of dye fluorescence at t=0, 100 and 200 ms after uncaging Ca^{2+}. The blue line shows the pathway on which fluorescent profiles are tracked and the ● indicates the center of the uncaging spot. (**B**) Time course of fluorescence changes along the dendritic pathway marked in **A**. The ▽ marks the time of photolysis. (**C**) Spatial profiles of fluorescence along the dendritic pathway indicated in **A**, centered on the uncaging spot. (**D**) The spatial variance of intracellular Ca^{2+} signals was linear over time for both smooth and spiny dendrites. (**E**) Logarithmic plots show normal diffusion of calcium (9 experiments in 8 cells).

NIH-PA Author Manuscript
NIH-PA Author Manuscript
NIH-PA Author Manuscript

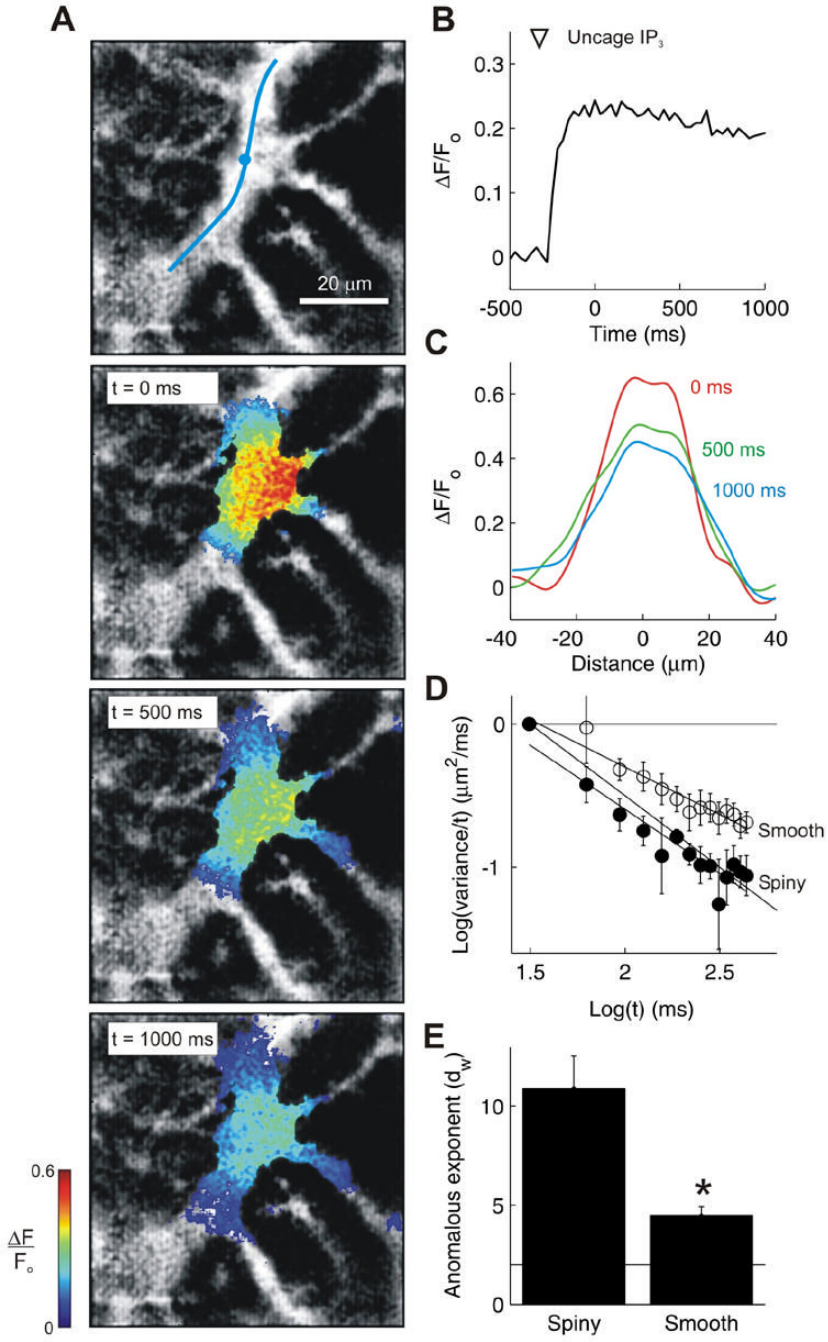

Figure 9.

IP_3 diffusion in Purkinje cell dendrites is regulated by both dendritic spines and cellular degradation. (**A**) Confocal images of a smooth dendrite and superimposed pseudocolor overlays of dye fluorescence at t=0, 500 and 1000 ms after uncaging IP_3. Blue line indicates pathway for fluorescence quantification and ● shows the center of the uncaging spot. (**B**) Time course of fluorescence changes along the dendritic pathway marked in **A**. The ▽ marks the time of photolysis of caged IP_3. (**C**) Spatial profiles of fluorescence changes along the dendritic pathway indicated in **A**, centered on the uncaging spot. (**D**) Logarithmic plots of average behavior of IP_3 signals, showing anomalous diffusion in smooth and spiny dendrites. (**E**) Mean

values for anomalous exponent in smooth and spiny dendrites (bars are the S.E.M.; 10 experiments in 8 cells). Asterisk indicates a significant difference between the two means ($p<0.01$, Mann-Whitney non-parametric test).

NIH-PA Author Manuscript
NIH-PA Author Manuscript
NIH-PA Author Manuscript